

TransERR: Translation-based Knowledge Graph Completion via Efficient Relation Rotation

Jiang Li^{1,2}, Xiangdong Su^{1,2}*

¹ College of Computer Science, Inner Mongolia University, Hohhot, China

² National & Local Joint Engineering Research Center of Intelligent Information Processing Technology for Mongolian, Hohhot, China
lijiangimu@gmail.com, cssxd@imu.edu.cn

Abstract

This paper presents translation-based knowledge graph completion method via efficient relation rotation (TransERR), a straightforward yet effective alternative to traditional translation-based knowledge graph completion models. Different from the previous translation-based models, TransERR encodes knowledge graphs in the hypercomplex-valued space, thus enabling it to possess a higher degree of translation freedom in mining latent information between the head and tail entities. To further minimize the translation distance, TransERR adaptively rotates the head entity and the tail entity with their corresponding unit quaternions, which are learnable in model training. The experiments on 7 benchmark datasets validate the effectiveness and the generalization of TransERR. The results also indicate that TransERR can better encode large-scale datasets with fewer parameters than the previous translation-based models. Our code is available at: <https://github.com/dellixx/TransERR>.

1 Introduction

Knowledge graphs (KGs), also known as semantic networks, represent networks of real-world entities (objects, events, concepts, etc.) and describe the associations between them. In fact, KGs contain factual triplets (*head, relation, tail*), which are denoted as (h, r, t) . Several open source KGs are available, including FreeBase (Bollacker et al., 2008), DBpedia (Lehmann et al., 2015) and NELL (Mitchell et al., 2018). They facilitate the development of downstream tasks, such as question answering (Chen et al., 2019), semantic search (Junior et al., 2020) and relation extraction (Hu et al., 2021). However, there is a problem with missing links in KGs. Therefore, knowledge graph completion (KGC) task has recently received considerable attention.

The mainstream approaches are to learn low-dimensional representations of entities and relations and utilize them to predict new facts. Most of them learn the embeddings of KGs based on score functions of the translational distance between the head and tail entities. TransE (Bordes et al., 2013), TransH (Wang et al., 2014), TransR (Lin et al., 2015) and TransD (Ji et al., 2015) adjust embeddings via different projection strategies to represent each relation as a translation vector r to connect head entity h and tail entity t in the real-valued space. Recently, to enrich the freedom of translation, RotatE (Sun et al., 2019) and Rotat3D (Gao et al., 2020) define each relation as a rotation from the head entity to the tail entity in the complex space and quaternion space, respectively.

Although the RotatE model has proven effective in modeling complex relational patterns in knowledge graphs, it is constrained by the limitation of being restricted to a single plane of rotation. While the recent Rotat3D model partially addresses this limitation by allowing for rotations in multiple planes, it still only provides one degree of freedom for relational rotation. To deal with above problem, PairRE (Chao et al., 2021), TripleRE (Yu et al., 2022), and TransSHER (Li et al., 2022) address the limitations of single-plane rotation by incorporating multiple relations to increase the degree of freedom for relational rotation. However, they are limited by rotation plane restrictions, which can lead to models that are not efficient in representing complex relational patterns.

To address this issue, we propose TransERR, which encodes knowledge graphs in the hypercomplex-valued space and utilizes two unit quaternion vectors to rotate the head entity and the tail entity, respectively. The unit quaternion vectors are learnable in model training, and they are highly to smooth rotation and spatial translation in the hypercomplex-valued vector space. In addition, two unit quaternion rotation vectors can

*Corresponding Author

further narrow the translation distance between the head and tail entities. As a result, TransERR possesses a higher degree of translation freedom in mining latent information between the head and tail entities. We evaluate the effectiveness and generalisation of our model on 7 KG benchmark datasets of different sizes. The experimental results show that TransERR significantly outperforms the existing state-of-the-art distance-based models.

2 Related Work

Translation Models. Translation-based models, also known as distance-based models. Motivated by the translation invariance in word2vec (Mikolov et al., 2013), TransE (Bordes et al., 2013) defines the distance between $h + r$ and t with the L_1 or L_2 norm constraint. After that, TransH (Wang et al., 2014), TransR (Lin et al., 2015) and TransD (Ji et al., 2015) employ different projection strategies to adjust graph embeddings. TransSparse (Ji et al., 2016) overcomes heterogeneity and imbalance by combining TransSparse (share) and TransSparse (separate). TransMS (Yang et al., 2019) performs multi-directional semantic transfer with non-linear functions and linear deviation vectors. RotatE (Sun et al., 2019) defines each relation as a rotation for a triplet from the head entity to the tail entity. Rotat3D (Gao et al., 2020) maps entities into 3D space and defines relations similar to RotatE. However, Rotat3D is limited by optimising the translation distance with only relation embedding information. Recently, PairRE (Chao et al., 2021), TripleRE (Yu et al., 2022) and TransHER (Li et al., 2022) employ multiple relations to improve the degree of freedom for relational rotation. Different from previous work, TransERR processes a high degree of rotation in the quaternion space. Benefiting from our model structure, TransERR allows for better optimization of the translation distance between entities, and thus better mine the latent information.

Semantic Matching Models. Semantic matching models mine possible semantic associations between entities and relations. The RESCAL (Nickel et al., 2011) represents each relation as a non-singular matrix. DistMult (Yang et al., 2014) uses a diagonal matrix rather than a non-singular matrix to address the problem of the excessive number of parameters in RESCAL. ComplEx (Trouillon et al., 2016) introduces complex-valued spaces into the KGs. TuckER (Balažević et al., 2019) employs Tucker decomposition of a binary tensor to

model a KG. Simple⁺ (Fatemi et al., 2019) extends Simple (Kazemi and Poole, 2018) and focus on encoding the subrelation pattern. QuatE (Zhang et al., 2019) takes advantage of quaternion representations to enable rich interactions between entities and relations. Deep neural networks have received a great deal of attention in recent years, e.g., ConvE (Dettmers et al., 2018a), ConvKB (Nguyen et al., 2018), InteractE (Vashishth et al., 2020) and R-GCNs (Schlichtkrull et al., 2018). However, they are difficult to analyze as they work as a black box.

3 Background and Notation

Link Prediction. A knowledge graph is usually described as $\mathcal{G} = (\mathcal{E}, \mathcal{R}, \mathcal{T})$, where \mathcal{E} , \mathcal{R} and \mathcal{T} denote the set of entities, relations and triplets (h, r, t) , respectively. Specifically, given $(h, r, ?)$, link prediction is to predict the tail entity in the triplet. Alternatively, given $(?, r, t)$, the task is to predict the head entity. The existing predicting models calculate the score function $f_r(h, t)$ and expect that the scores of correct triplets are higher than those of invalid triplets.

Quaternion Algebra. The quaternion is an extension of the complex number in the four-dimensional space. It consists of a real part and three imaginary parts, which is proposed by William Rowan Hamilton (Hamilton, 1844). A quaternion q is defined as $q = a + bi + cj + dk$, where a is real unit and i, j, k are three imaginary units. In addition, $i^2 = j^2 = k^2 = ijk = -1$.

- The unit quaternion q^\triangleleft is defined as

$$q^\triangleleft = \frac{a + bi + cj + dk}{\sqrt{a^2 + b^2 + c^2 + d^2}}. \quad (1)$$

- Hamilton product of two quaternions is

$$\begin{aligned} q_1 \otimes q_2 = & (a_1a_2 - b_1b_2 - c_1c_2 - d_1d_2) + \\ & (a_1b_2 + b_1a_2 + c_1d_2 - d_1c_2)i + \\ & (a_1c_2 - b_1d_2 + c_1a_2 + d_1b_2)j + \\ & (a_1d_2 + b_1c_2 - c_1b_2 + d_1a_2)k. \end{aligned} \quad (2)$$

4 Methodology

4.1 TransERR

Quaternions enable expressive rotation in the hypercomplex-valued space and have more degree of freedom than translation in the real-valued

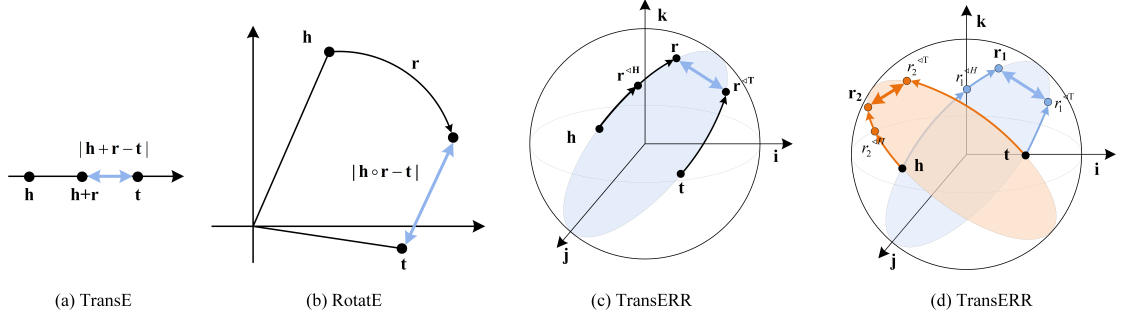


Figure 1: Illustration of TransE, RotatE and TransERR. TransE, RotatE and TransERR encode knowledge graphs in the real-valued space, complex-valued space and hypercomplex-valued space, respectively. \circ denotes Hadamard product. The distance function of TransERR is $\| \mathbf{h} \otimes \mathbf{r}^{\langle \mathbf{H} \rangle} + \mathbf{r} - \mathbf{t} \otimes \mathbf{r}^{\langle \mathbf{T} \rangle} \|$.

space. Hence, to obtain a greater degree of translation freedom in the link prediction, TransERR encodes knowledge graphs in the hypercomplex-valued space. In addition, we rotate head entity \mathbf{h} and tail entity \mathbf{t} via two unit quaternion vectors $\mathbf{r}^{\langle \mathbf{H} \rangle}$ and $\mathbf{r}^{\langle \mathbf{T} \rangle}$, as shown in Figure 1. Unlike TransE and RotatE, TransERR utilizes Hamilton product \otimes rather than Hadamard product \circ in project operation to better capture the underlying semantic features between the head entity and the tail entity embeddings. Firstly, given a triplet (h, r, t) , we encode h, r and t in the quaternion space, which are denoted as

$$\begin{aligned} \mathbf{h} &= \mathbf{a}_h + \mathbf{b}_h i + \mathbf{c}_h j + \mathbf{d}_h k \\ \mathbf{r} &= \mathbf{a}_r + \mathbf{b}_r i + \mathbf{c}_r j + \mathbf{d}_r k \\ \mathbf{t} &= \mathbf{a}_t + \mathbf{b}_t i + \mathbf{c}_t j + \mathbf{d}_t k, \end{aligned} \quad (3)$$

where $\mathbf{h}, \mathbf{r}, \mathbf{t} \in \mathbb{H}^d$, $\mathbf{a}_h, \mathbf{b}_h, \mathbf{c}_h, \mathbf{d}_h \in \mathbb{R}^{\frac{d}{4}}$, $\mathbf{a}_r, \mathbf{b}_r, \mathbf{c}_r, \mathbf{d}_r \in \mathbb{R}^{\frac{d}{4}}$ and $\mathbf{a}_t, \mathbf{b}_t, \mathbf{c}_t, \mathbf{d}_t \in \mathbb{R}^{\frac{d}{4}}$. Next, we define two additional quaternion vectors to rotate the head and tail entity, which are represented as $\mathbf{r}^{\mathbf{H}}$ and $\mathbf{r}^{\mathbf{T}}$, where $\mathbf{r}^{\mathbf{H}}$ and $\mathbf{r}^{\mathbf{T}} \in \mathbb{H}^d$. Then, we normalize these two additional quaternions ($\mathbf{r}^{\mathbf{H}}$ and $\mathbf{r}^{\mathbf{T}}$) to the unit quaternions ($\mathbf{r}^{\langle \mathbf{H} \rangle}$ and $\mathbf{r}^{\langle \mathbf{T} \rangle}$) to eliminate the scaling effect. They are denoted as

$$\begin{aligned} \mathbf{r}^{\langle \mathbf{H} \rangle} &= \frac{\mathbf{a}_{r^{\mathbf{H}}} + \mathbf{b}_{r^{\mathbf{H}}} i + \mathbf{c}_{r^{\mathbf{H}}} j + \mathbf{d}_{r^{\mathbf{H}}} k}{\sqrt{\mathbf{a}_{r^{\mathbf{H}}}^2 + \mathbf{b}_{r^{\mathbf{H}}}^2 + \mathbf{c}_{r^{\mathbf{H}}}^2 + \mathbf{d}_{r^{\mathbf{H}}}^2}} \\ \mathbf{r}^{\langle \mathbf{T} \rangle} &= \frac{\mathbf{a}_{r^{\mathbf{T}}} + \mathbf{b}_{r^{\mathbf{T}}} i + \mathbf{c}_{r^{\mathbf{T}}} j + \mathbf{d}_{r^{\mathbf{T}}} k}{\sqrt{\mathbf{a}_{r^{\mathbf{T}}}^2 + \mathbf{b}_{r^{\mathbf{T}}}^2 + \mathbf{c}_{r^{\mathbf{T}}}^2 + \mathbf{d}_{r^{\mathbf{T}}}^2}}. \end{aligned} \quad (4)$$

The normalized operation ensures the stability of entity rotation in the quaternion space. The unit quaternion vectors are highly desirable to smooth

rotation and spatial translation in the hypercomplex-valued space. In addition, two unit quaternion rotation vectors can further narrow the translation distance between the head and tail entities. Finally, we employ $\mathbf{r}^{\langle \mathbf{H} \rangle}$ and $\mathbf{r}^{\langle \mathbf{T} \rangle}$ to rotate head entity \mathbf{h} and tail entity \mathbf{t} , respectively. Specifically, we use Hamilton product to achieve rotation operation since Hamilton product makes quaternion more expressive at rotational capability. For each triplet (h, r, t) , we define the distance function of TransERR as

$$d_r(\mathbf{h}, \mathbf{t}) = \| \mathbf{h} \otimes \mathbf{r}^{\langle \mathbf{H} \rangle} + \mathbf{r} - \mathbf{t} \otimes \mathbf{r}^{\langle \mathbf{T} \rangle} \| . \quad (5)$$

The score function $f_r(\mathbf{h}, \mathbf{t}) = -d_r(\mathbf{h}, \mathbf{t})$ and \otimes is defined in Section 3. Following Sun et al. (2019), we employ the self-adversarial negative sampling loss for TransERR, which is defined as

$$\begin{aligned} \mathcal{L} &= -\log \sigma(\gamma - d_r(\mathbf{h}, \mathbf{t})) \\ &- \sum_{i=1}^n p(h'_i, r, t'_i) \log \sigma(d_r(\mathbf{h}'_i, \mathbf{t}'_i) - \gamma), \end{aligned} \quad (6)$$

where σ is the sigmoid function, and γ is a fixed margin. (h'_i, r, t'_i) and $d_r(\mathbf{h}'_i, \mathbf{t}'_i)$ represent the i -th negative triplet and the distance function of the i -th negative triplet.

5 Experimental Setup

5.1 Datasets

We utilize the 7 most commonly utilized link prediction datasets and validate the effectiveness and generalizability of TransERR. We summarise the details of datasets in Table 2. ogbl-wikikg2 (Hu et al., 2020) is a very large-scale dataset extracted from the Wikidata knowledge base (Vrandečić and

ogbl-wikikg2					
	#Dim	#Params	Test MRR	Valid MRR	
TransE	500	1250.57M	0.4256 ± 0.0030	0.4272 ± 0.0030	
DistMult	500	1250.57M	0.3729 ± 0.0045	0.3506 ± 0.0042	
ComplEx	250	1250.44M	0.4027 ± 0.0027	0.3759 ± 0.0016	
RotatE	250	1250.44M	0.4332 ± 0.0025	0.4353 ± 0.0028	
PairRE	200	500.33M	0.5208 ± 0.0027	0.5423 ± 0.0020	
TripleRE	200	500.76M	0.5794 ± 0.0020	0.6045 ± 0.0024	
TransERR (ours)	100	250.22M	<u>0.6100</u> ± 0.0020	<u>0.6246</u> ± 0.0019	
TransERR (ours)	200	500.44M	0.6359 ± 0.0020	0.6518 ± 0.0011	

Table 1: Results on ogbl-wikikg2. Results are taken from official leaderboard (Hu et al., 2020). Best results are in bold.

Dataset	$ \mathcal{E} $	$ \mathcal{R} $	#Train	#Valid	#Test
ogbl-wikikg2	2,500k	535	16,109k	429k	598k
YAGO3-10	123k	37	1,079k	5k	5k
DB100K	100k	470	597k	50k	50k
FB15K	15k	237	483k	50k	50k
WN18	41k	18	141k	5k	5k
FB15K-237	15k	237	272k	18k	20k
WN18RR	41k	11	87k	3k	3k

Table 2: Statistics of the datasets in the experiment.

Kröttsch, 2014). YAGO3-10 (Suchanek et al., 2007) is a subset of YAGO3, which are mainly from Wikipedia. DB100k (Ding et al., 2018) is a subset of DBpedia. FB15K (Bordes et al., 2013) is a subset of the Freebase knowledge base, while FB15k-237 (Toutanova and Chen, 2015) removes the inversion relations from FB15K. WN18 (Bordes et al., 2013) is extracted from WordNet (Miller, 1995). WN18RR (Dettmers et al., 2018b) removes inversion relations similar to FB15K-237.

5.2 Evaluation Protocol

Following the SOTA methods (Sun et al., 2019; Chao et al., 2021), the quality of the ranking of each test triplet is evaluated via calculating all possible substitutions of head entity and tail entity : (h', r, t) and (h, r, t') , where $h', t' \in \mathcal{E}$. We evaluate the performance using the standard evaluation metrics, including Mean Rank (MR), Mean Reciprocal Rank (MRR) and Hits@N. Hits@N measures the percentage of correct entities in the top n predictions. Higher values of MRR and Hits@N indicate better performance. Nevertheless, MR is the exact opposite of MRR and Hits@n. Hits@N ratio with cut-off values $N = 1, 3, 10$. For experi-

ments on ogbl-wikikg2, we follow the evaluation protocol of ogbl-wikikg2 benchmarks (Hu et al., 2020). Other experimental setups can be found in the Appendix A.

5.3 Implementation

We implement our proposed model via pytorch. We use Adam (Kingma and Ba, 2014) optimizer, and employ grid search to find the best hyperparameters based on the performance on the validation datasets. We report averaged test results across ten runs and use the random seeds from 0 to 9. We omit the variance as it is generally low. We employ the official implementations (Hu et al., 2020) for ogbl-wikikg2 ¹.

6 Results and Analysis

6.1 Main Results

To evaluate the effectiveness and the generalization of TransERR, we perform the experiments on 7 benchmark datasets of different scales. The results on ogbl-wikikg2 are shown in Table 1. TransERR achieves competitive results on large-scale datasets. On ogbl-wikikg2, TransERR obtains significant improvements of 9.7% than TripleRE with the same number of parameters (#Dim 200) in Test MRR. It is worth noting that TransERR still outperforms PairRE, TripleRE with fewer parameters (#Dim 100). The results demonstrate that TransERR has a powerful capability to model large-scale KGs.

The comparison results for WN18RR and FB15K-237 are shown in Table 3. TransERR outperforms all the baselines in all metrics on

¹<https://ogb.stanford.edu/>

	WN18RR					FB15K-237				
	MR	MRR	Hits@10	Hits@3	Hits@1	MR	MRR	Hits@10	Hits@3	Hits@1
TransE ♡	3384	0.266	0.501	-	-	357	0.294	0.465	-	-
DistMult ♡	5110	0.43	0.49	0.44	0.39	254	0.241	0.419	0.263	0.155
ComplEx ♡	5261	0.44	0.51	0.46	0.41	339	0.247	0.428	0.275	0.158
TuckER	-	0.470	0.526	0.482	0.443	-	0.358	0.544	0.394	0.266
RotatE ♡	3340	0.476	0.571	0.492	0.428	177	0.338	0.533	0.375	0.241
Rotat3D	3328	0.489	0.579	0.505	0.442	165	0.347	0.543	0.385	0.250
QuatE	3472	0.481	0.564	0.500	0.436	176	0.311	0.495	0.342	0.221
ATTH	-	0.466	0.551	0.484	0.419	-	0.324	0.501	0.354	0.236
Rot_Pro	2815	0.457	0.557	0.482	0.397	201	0.344	0.540	0.383	0.246
PairRE	-	-	-	-	-	160	0.351	0.544	0.387	0.256
TripleRE	-	-	-	-	-	142	0.351	0.544	0.387	0.256
TransSHER	-	-	-	-	-	-	0.360	0.551	0.397	0.264
TransERR	1167	0.501	0.605	0.520	0.450	125	0.360	0.555	0.396	0.264

Table 3: Results on WN18RR and FB15K-237. Results of ♡ are taken from Sun et al. (2019). The best results are in bold. The dashes means that the results are not reported in the responding literature.

Scoring Function	FB15K		FB15K-237		WN18		WN18RR	
	MRR	Hits@10	MRR	Hits@10	MRR	Hits@10	MRR	Hits@10
$- \ \mathbf{h} \circ \mathbf{r}^{\mathbf{H}} + \mathbf{r} - \mathbf{t} \circ \mathbf{r}^{\mathbf{T}} \ $	0.391	0.561	0.235	0.419	0.909	0.944	0.469	0.563
$- \ \mathbf{h} \circ \mathbf{r}^{\langle \mathbf{H} \rangle} + \mathbf{r} - \mathbf{t} \circ \mathbf{r}^{\langle \mathbf{T} \rangle} \ $	0.732	0.860	0.352	0.537	0.921	0.963	0.481	0.580
$- \ \mathbf{h} \otimes \mathbf{r}^{\mathbf{H}} + \mathbf{r} - \mathbf{t} \otimes \mathbf{r}^{\mathbf{T}} \ $	0.425	0.598	0.290	0.454	0.950	0.961	0.492	0.586
$- \ \mathbf{h} \otimes \mathbf{r}^{\langle \mathbf{H} \rangle} + \mathbf{r} - \mathbf{t} \otimes \mathbf{r}^{\langle \mathbf{T} \rangle} \ $	0.815	0.896	0.360	0.555	0.953	0.965	0.501	0.605

Table 4: Ablation of TransERR on FB15K, FB15K-237, WN18 and WN18RR. \circ and \otimes are Hadamard product and Hamilton product, respectively. $\mathbf{r}^{\langle \mathbf{H} \rangle}$ and $\mathbf{r}^{\langle \mathbf{T} \rangle}$ are normalized complex vectors. $\mathbf{r}^{\mathbf{H}}$ and $\mathbf{r}^{\mathbf{T}}$ are normalized quaternion vectors.

WN18RR. Compared with RotatE, TransERR achieves improvements of 65.0%, 5.2%, 5.9%, 5.6% and 5.1%, respectively. For FB15K-237, TransERR gains competitive results than existing distance-based models in MR, MRR, Hit@10 and Hits@3. The above results confirm that TransERR has merit in modeling graph embeddings and improves the link prediction performance. This is because quaternions enable expressive rotation in the hypercomplex-valued space, and two unit quaternion vectors further narrow the translation distance between the head and tail entities. Please refer to Appendix B for additional dataset results.

6.2 Ablation Study

In this part, in order to demonstrate TransERR can better capture latent information between entity embeddings in the hypercomplex-valued space than in the complex-valued space, we encode TransERR in the complex space and conduct experiments

on FB15K, FB15K-237, WN18 and WN18RR. As shown in the second and fourth rows of Table 4, we can observe that TransERR behaves better in the quaternion space. This is further evidence that TransERR can facilitate interaction information between the head and tail entities in the hypercomplex-valued space. Furthermore, we conduct an ablation study on quaternion normalization for TransERR, where rows one and two are a control group and rows three and four are a control group in Table 4. We remove the normalization step for $\mathbf{r}^{\mathbf{H}}$ and $\mathbf{r}^{\mathbf{T}}$ and utilize $\mathbf{r}^{\mathbf{H}}$ and $\mathbf{r}^{\mathbf{T}}$ to rotate head entities and tail entities in the complex-valued space and in the hypercomplex-valued space, respectively. We conclude that the relational rotation’s geometric property is lost, leading to poor performance. In addition, the unit quaternion has a high degree of smooth rotation and spatial transformation ability than the unit complex number.

7 Conclusion

This paper proposes a simple yet effective distance-based KGC model (TransERR), which rotates entities with two normalized quaternion vectors in the hypercomplex-valued space. TransERR possesses a higher degree of translation freedom for graph embeddings. The experiments also suggest that TransERR can maximize interaction information between entities in the hypercomplex-valued space. The experimental results fully illustrate the effectiveness and generalizability of our model. In addition, the results show that two unit quaternions can further narrow the distance between the head and tail entities, and thus avoid information loss in rotation.

References

- Ivana Balažević, Carl Allen, and Timothy Hospedales. 2019. Tucker: Tensor factorization for knowledge graph completion. In *Proceedings of the 2019 Conference on Empirical Methods in Natural Language Processing and the 9th International Joint Conference on Natural Language Processing (EMNLP-IJCNLP)*, pages 5185–5194.
- Kurt Bollacker, Colin Evans, Praveen Paritosh, Tim Sturge, and Jamie Taylor. 2008. Freebase: a collaboratively created graph database for structuring human knowledge. In *Proceedings of the 2008 ACM SIGMOD international conference on Management of data*, pages 1247–1250.
- Antoine Bordes, Nicolas Usunier, Alberto Garcia-Duran, Jason Weston, and Oksana Yakhnenko. 2013. Translating embeddings for modeling multi-relational data. *Advances in neural information processing systems*, 26.
- Linlin Chao, Jianshan He, Taifeng Wang, and Wei Chu. 2021. Pairre: Knowledge graph embeddings via paired relation vectors. In *Proceedings of the 59th Annual Meeting of the Association for Computational Linguistics and the 11th International Joint Conference on Natural Language Processing (Volume 1: Long Papers)*, pages 4360–4369.
- Yu Chen, Lingfei Wu, and Mohammed J Zaki. 2019. Bidirectional attentive memory networks for question answering over knowledge bases. *arXiv preprint arXiv:1903.02188*.
- Tim Dettmers, Pasquale Minervini, Pontus Stenetorp, and Sebastian Riedel. 2018a. Convolutional 2d knowledge graph embeddings. In *Thirty-second AAAI conference on artificial intelligence*.
- Tim Dettmers, Pasquale Minervini, Pontus Stenetorp, and Sebastian Riedel. 2018b. Convolutional 2d knowledge graph embeddings. In *Thirty-second AAAI conference on artificial intelligence*.
- Boyang Ding, Quan Wang, Bin Wang, and Li Guo. 2018. Improving knowledge graph embedding using simple constraints. In *Proceedings of the 56th Annual Meeting of the Association for Computational Linguistics (Volume 1: Long Papers)*, pages 110–121.
- Bahare Fatemi, Siamak Ravanbakhsh, and David Poole. 2019. Improved knowledge graph embedding using background taxonomic information. In *Proceedings of the AAAI Conference on Artificial Intelligence*, volume 33, pages 3526–3533.
- Chang Gao, Chengjie Sun, Lili Shan, Lei Lin, and Mingjiang Wang. 2020. Rotate3d: Representing relations as rotations in three-dimensional space for knowledge graph embedding. In *Proceedings of the 29th ACM International Conference on Information & Knowledge Management*, pages 385–394.
- Wm R Hamilton. 1844. Theory of quaternions. *Proceedings of the Royal Irish Academy (1836-1869)*, 3:1–16.
- Weihua Hu, Matthias Fey, Marinka Zitnik, Yuxiao Dong, Hongyu Ren, Bowen Liu, Michele Catasta, and Jure Leskovec. 2020. Open graph benchmark: Datasets for machine learning on graphs. *Advances in neural information processing systems*, 33:22118–22133.
- Zikun Hu, Yixin Cao, Lifu Huang, and Tat-Seng Chua. 2021. How knowledge graph and attention help? a quantitative analysis into bag-level relation extraction. *arXiv preprint arXiv:2107.12064*.
- Guoliang Ji, Shizhu He, Liheng Xu, Kang Liu, and Jun Zhao. 2015. Knowledge graph embedding via dynamic mapping matrix. In *Proceedings of the 53rd Annual Meeting of the Association for Computational Linguistics and the 7th International Joint Conference on Natural Language Processing (Volume 1: Long Papers)*, pages 687–696.
- Guoliang Ji, Kang Liu, Shizhu He, and Jun Zhao. 2016. Knowledge graph completion with adaptive sparse transfer matrix. In *Thirtieth AAAI conference on artificial intelligence*.
- Ademar Crotti Junior, Fabrizio Orlandi, Damien Graux, Murhaf Hossari, Declan O’Sullivan, Christian Hartz, and Christian Dirschl. 2020. Knowledge graph-based legal search over german court cases. In *European Semantic Web Conference*, pages 293–297. Springer.
- Seyed Mehran Kazemi and David Poole. 2018. Simple embedding for link prediction in knowledge graphs. *Advances in neural information processing systems*, 31.
- Diederik P Kingma and Jimmy Ba. 2014. Adam: A method for stochastic optimization. *arXiv preprint arXiv:1412.6980*.
- Jens Lehmann, Robert Isele, Max Jakob, Anja Jentzsch, Dimitris Kontokostas, Pablo N Mendes, Sebastian Hellmann, Mohamed Morsey, Patrick Van Kleef,

- Sören Auer, et al. 2015. Dbpedia—a large-scale, multilingual knowledge base extracted from wikipedia. *Semantic web*, 6(2):167–195.
- Yizhi Li, Wei Fan, Chao Liu, Chenghua Lin, and Jiang Qian. 2022. **TranSHER: Translating knowledge graph embedding with hyper-ellipsoidal restriction**. In *Proceedings of the 2022 Conference on Empirical Methods in Natural Language Processing*, pages 8517–8528, Abu Dhabi, United Arab Emirates. Association for Computational Linguistics.
- Yankai Lin, Zhiyuan Liu, Maosong Sun, Yang Liu, and Xuan Zhu. 2015. Learning entity and relation embeddings for knowledge graph completion. In *Twenty-ninth AAAI conference on artificial intelligence*.
- Tomas Mikolov, Kai Chen, Greg Corrado, and Jeffrey Dean. 2013. Efficient estimation of word representations in vector space. *arXiv preprint arXiv:1301.3781*.
- George A Miller. 1995. Wordnet: a lexical database for english. *Communications of the ACM*, 38(11):39–41.
- Tom Mitchell, William Cohen, Estevam Hruschka, Partha Talukdar, Bishan Yang, Justin Betteridge, Andrew Carlson, Bhavana Dalvi, Matt Gardner, Bryan Kisiel, et al. 2018. Never-ending learning. *Communications of the ACM*, 61(5):103–115.
- Tu Dinh Nguyen, Dat Quoc Nguyen, Dinh Phung, et al. 2018. A novel embedding model for knowledge base completion based on convolutional neural network. In *Proceedings of the 2018 Conference of the North American Chapter of the Association for Computational Linguistics: Human Language Technologies, Volume 2 (Short Papers)*, pages 327–333.
- Maximilian Nickel, Volker Tresp, and Hans-Peter Kriegel. 2011. A three-way model for collective learning on multi-relational data. In *ICML*.
- Michael Schlichtkrull, Thomas N Kipf, Peter Bloem, Rianne van den Berg, Ivan Titov, and Max Welling. 2018. Modeling relational data with graph convolutional networks. In *European semantic web conference*, pages 593–607. Springer.
- Fabian M Suchanek, Gjergji Kasneci, and Gerhard Weikum. 2007. Yago: a core of semantic knowledge. In *Proceedings of the 16th international conference on World Wide Web*, pages 697–706.
- Zhiqing Sun, Zhi-Hong Deng, Jian-Yun Nie, and Jian Tang. 2019. Rotate: Knowledge graph embedding by relational rotation in complex space. *arXiv preprint arXiv:1902.10197*.
- Kristina Toutanova and Danqi Chen. 2015. Observed versus latent features for knowledge base and text inference. In *Proceedings of the 3rd workshop on continuous vector space models and their compositionality*, pages 57–66.
- Théo Trouillon, Johannes Welbl, Sebastian Riedel, Éric Gaussier, and Guillaume Bouchard. 2016. Complex embeddings for simple link prediction. In *International conference on machine learning*, pages 2071–2080. PMLR.
- Shikhar Vashishth, Soumya Sanyal, Vikram Nitin, Nilesh Agrawal, and Partha Talukdar. 2020. Interact: Improving convolution-based knowledge graph embeddings by increasing feature interactions. In *Proceedings of the AAAI Conference on Artificial Intelligence*, volume 34, pages 3009–3016.
- Denny Vrandečić and Markus Krötzsch. 2014. **Wiki-data: A free collaborative knowledgebase**. *Commun. ACM*, 57(10):78–85.
- Zhen Wang, Jianwen Zhang, Jianlin Feng, and Zheng Chen. 2014. Knowledge graph embedding by translating on hyperplanes. In *Proceedings of the AAAI Conference on Artificial Intelligence*, volume 28.
- Bishan Yang, Wen-tau Yih, Xiaodong He, Jianfeng Gao, and Li Deng. 2014. Embedding entities and relations for learning and inference in knowledge bases. *arXiv preprint arXiv:1412.6575*.
- Shihui Yang, Jidong Tian, Honglun Zhang, Junchi Yan, Hao He, and Yaohui Jin. 2019. Transms: Knowledge graph embedding for complex relations by multidirectional semantics. In *IJCAI*, pages 1935–1942.
- Long Yu, Zhicong Luo, Huanyong Liu, Deng Lin, Hongzhu Li, and Yafeng Deng. 2022. Triplere: Knowledge graph embeddings via tripled relation vectors. *arXiv preprint arXiv:2209.08271*.
- Shuai Zhang, Yi Tay, Lina Yao, and Qi Liu. 2019. Quaternion knowledge graph embeddings. *Advances in neural information processing systems*, 32.

A Hyperparameters

We list the best hyperparameters setting of TransERR on 7 benchmark datasets in Table 5. d , ϵ , n , α and γ denote the embedding size, the learning rate, the negative sample, the self-adversarial sampling temperature and fixed margin, respectively. In general, the embedding size d is tuned amongst $\{100, 200, 500, 1000, 1500, 2000\}$, the learning rate ϵ is tuned amongst $\{1e^{-3}, 5e^{-4}, 1e^{-4}, 5e^{-5}, 1e^{-5}\}$, the negative sample n is selected in $\{128, 256\}$, the self-adversarial sampling temperature α is selected from $\{0.5, 1\}$, the fixed margin γ are searched from 5 to 30. All optimal hyperparameters are selected on the validation set.

Benchmark	embedding dimension d	learning rate ϵ	negative sample n	α	γ
ogbl-wikikg2	200	$1e^{-3}$	128	1.0	15
ogbl-wikikg2	100	$1e^{-3}$	128	1.0	8
YAGO3-10	1000	$5e^{-4}$	256	0.5	30
DB100K	1000	$1e^{-4}$	128	0.5	20
FB15K	1500	$1e^{-4}$	256	1.0	26
WN18	1000	$1e^{-3}$	128	0.5	10
FB15K-237	1000	$1e^{-3}$	128	0.5	20
WN18RR	1000	$1e^{-3}$	128	0.5	12

Table 5: The best hyperparameter setting of TransERR on 10 benchmarks datasets.

B Additional Dataset Results

The comparison results for WN18 and FB15K are shown in Table 6. We employ the same hyperparameter settings and implementation compared with the previous works. Since both the baselines and TransERR almost obtains the upper bound on Hits@N, the improvement of TransERR is still considered effective. We can see that TransERR achieves significant improvements on WN18 and FB15K.

The results on YAGO3-10 and DB100K datasets are shown in Table 7. TransERR achieves the best results in all metrics for YAGO3-10. On DB100K, compared with the latest TranSHER, TransERR produces the optimal performance in all metrics except MR, which obtains significant improvements of 7.8%, 5.6%, 7.1% and 10.1%, respectively.

	WN18					FB15K				
	MR	MRR	Hits@10	Hits@3	Hits@1	MR	MRR	Hits@10	Hits@3	Hits@1
TransE ♡	-	0.495	0.943	0.888	0.111	-	0.463	0.749	0.578	0.297
DistMult ♡	665	0.797	0.946	-	-	42	0.798	0.893	-	-
ComplEx ♡	-	0.941	0.947	0.945	0.936	-	0.692	0.840	0.759	0.599
TuckER	-	0.953	0.958	0.955	0.949	-	0.795	0.892	0.833	0.741
RotatE ♡	309	0.949	0.959	0.952	0.944	40	0.797	0.884	0.830	0.746
Rotat3D	214	0.951	0.961	0.953	0.945	39	0.789	0.887	0.835	0.728
QuatE	338	0.949	0.960	0.954	0.941	41	0.770	0.878	0.821	0.700
PairRE	401	0.941	0.956	0.950	0.940	37	0.811	0.896	0.845	0.765
TripleRE	-	-	-	-	-	35	0.747	0.877	0.813	0.662
TransERR	82	0.953	0.965	0.957	0.945	41	0.815	0.896	0.848	0.767

Table 6: Results on WN18 and FB15K. Results of ♡ are taken from Sun et al. (2019). Other results are taken from the corresponding original papers. The best results are in bold. The dashes means that the results are not reported in the responding literature.

	YAGO3-10					DB100K				
	MR	MRR	Hits@10	Hits@3	Hits@1	MR	MRR	Hits@10	Hits@3	Hits@1
TransE	-	-	-	-	-	-	0.111	0.270	0.164	0.016
DistMult	5926	0.34	0.54	0.38	0.24	-	0.233	0.448	0.301	0.115
ComplEx	6351	0.36	0.55	0.40	0.26	-	0.242	0.440	0.312	0.126
ConvE	1671	0.44	0.62	0.49	0.35	-	-	-	-	-
Rot_Pro	1797	0.542	0.699	0.596	0.443	-	-	-	-	-
PairRE	-	-	-	-	-	-	0.412	0.600	0.472	0.309
TransSHER	-	-	-	-	-	-	0.431	0.589	0.476	0.345
TransERR	476	0.546	0.706	0.601	0.456	571	0.465	0.622	0.510	0.380

Table 7: Results on YAGO3-10 and DB100K. Results are taken from the corresponding original papers. The best results are in bold. The dashes means that the results are not reported in the responding literature.